Adipocyte-secreted exosomal microRNA-34a inhibits M2 macrophage polarization to promote obesity-induced adipose inflammation

Yong Pan,[1,2] Xiaoyan Hui,[1,2] Ruby Lai Chong Hoo,[1,3] Dewei Ye,[4,5] Cyrus Yuk Cheung Chan,[1,2] Tianshi Feng,[1,3] Yu Wang,[1,3] Karen Siu Ling Lam,[1,2] and Aimin Xu[1,2,3]

[1]State Key Laboratory of Pharmaceutical Biotechnology, [2]Department of Medicine, and [3]Department of Pharmacy and Pharmacology, The University of Hong Kong, Hong Kong, China. [4]Joint Laboratory between Guangdong and Hong Kong on Metabolic Diseases, Guangdong Pharmaceutical University, Guangzhou, China. [5]Guangdong Research Center of Metabolic Diseases of Integrated Western and Chinese Medicine, Guangdong Pharmaceutical University, Guangzhou, China.

Persistent, unresolved inflammation in adipose tissue is a major contributor to obesity-associated metabolic complications. However, the molecular links between lipid-overloaded adipocytes and inflammatory immune cells in obese adipose tissues remain elusive. Here we identified adipocyte-secreted microRNA-34a (miR-34a) as a key mediator through its paracrine actions on adipose-resident macrophages. The expression of miR-34a in adipose tissues was progressively increased with the development of dietary obesity. Adipose-selective or adipocyte-specific miR-34a–KO mice were resistant to obesity-induced glucose intolerance, insulin resistance, and systemic inflammation, and this was accompanied by a significant shift in polarization of adipose-resident macrophages from proinflammatory M1 to antiinflammatory M2 phenotype. Mechanistically, mature adipocyte-secreted exosomes transported miR-34a into macrophages, thereby suppressing M2 polarization by repressing the expression of Krüppel-like factor 4 (Klf4). The suppressive effects of miR-34a on M2 polarization and its stimulation of inflammatory responses were reversed by ectopic expression of Klf4 in both bone marrow–derived macrophages and adipose depots of obese mice. Furthermore, increased miR-34a expression in visceral fat of overweight/obese subjects correlated negatively with reduced Klf4 expression, but positively with the parameters of insulin resistance and metabolic inflammation. In summary, miR-34a was a key component of adipocyte-secreted exosomal vesicles that transmitted the signal of nutrient overload to the adipose-resident macrophages for exacerbation of obesity-induced systemic inflammation and metabolic dysregulation.

Introduction

Adipose tissue is a highly dynamic metabolic organ that plays a central role in the regulation of energy homeostasis (1). Besides its role as a primary site for energy storage, adipose tissue controls glucose metabolism and systemic insulin sensitivity by secreting a large number of bioactive peptides (adipokines) and metabolites (such as sphingolipids). Chronic nutrient excess often results in the unhealthy expansion and remodeling of adipose tissue, leading to unresolved inflammation, which is a major culprit in obesity-related cardiometabolic comorbidities as well as neurodegenerative disorders (2). Data from both animal studies and clinical investigations suggest that "inflamed" adipose tissue (especially visceral fat) is a predominant contributor to systemic, low-grade inflammation associated with obesity. Adipose-selective ablation of the major inflammatory pathways (such as JNK and NF-κB) is sufficient to counteract obesity-related systemic inflammation, insulin resistance, and metabolic dysregulation (3, 4).

During the progression of obesity, expansion of adipose tissue causes infiltration and activation of immune cells involved in both innate and adaptive immunity, which in turn elicit a series of acute and chronic inflammatory responses within the tissue. While acute inflammation at the early stage of obesity may serve as an adaptive response required for appropriate adipose tissue expansion and storage of toxic lipids, unresolved chronic inflammation in adipose tissue causes a series of detrimental consequences for cardiometabolic health. Among adipose-resident immune cells, macrophages are the most abundant cell type, constituting up to 50% of total cells of adipose tissue in obesity (5). Increased infiltration of macrophages is observed in adipose tissue from both obese mice and human subjects, where they form crown-like structures (CLSs) surrounding dying or dead adipocytes (6). The number of adipose tissue–resident macrophages (ATMs) is tightly linked to the degree of insulin resistance and metabolic dysregulation, whereas selective depletion of ATMs by either genetic or pharmacological approaches is adequate to reverse insulin resistance and glucose intolerance in obese mice (5, 7).

Macrophages are highly plastic in nature, exhibiting different phenotypes ranging from the classically activated, proinflammatory M1 to alternatively activated, antiinflammatory

Conflict of interest: The authors have declared that no conflict of interest exists.

Submitted: June 22, 2018; **Accepted:** November 27, 2018.
Reference information: *J Clin Invest*. 2019;129(2):834–849.
https://doi.org/10.1172/JCI123069.

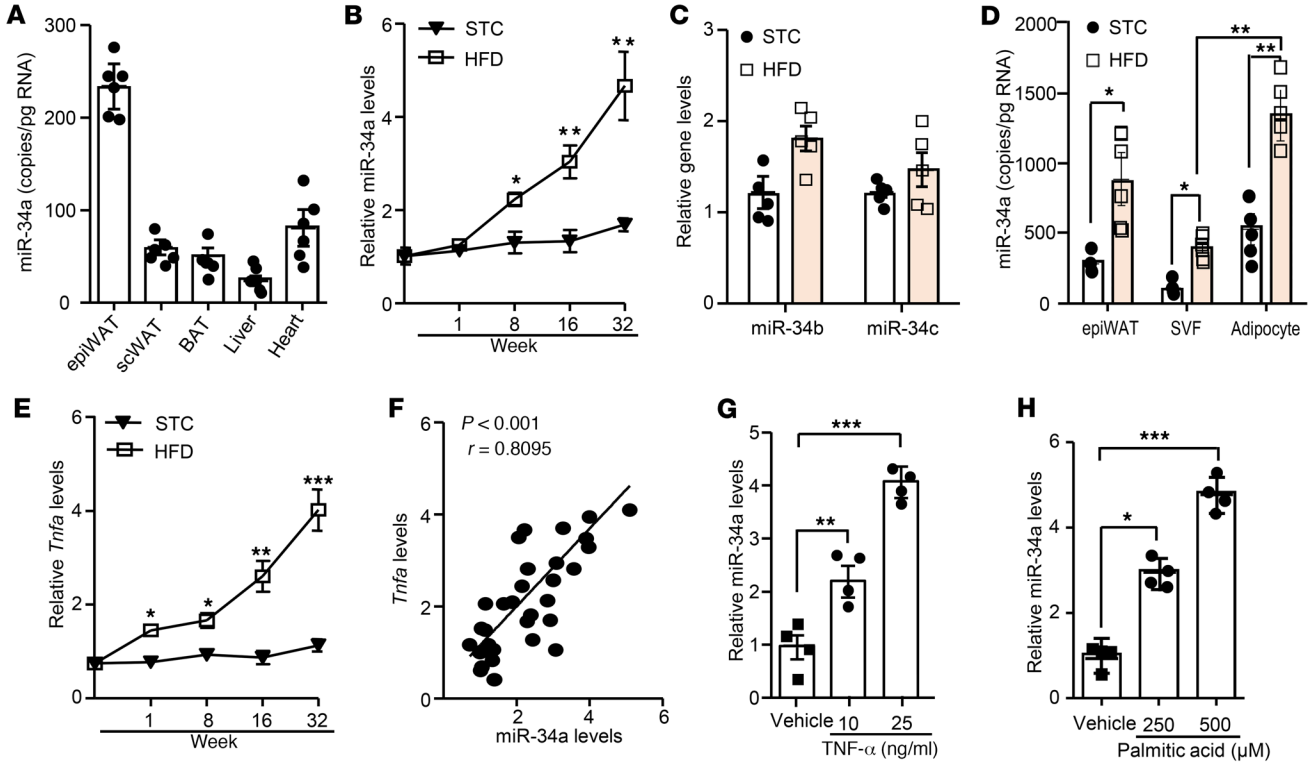

Figure 1. MiR-34a is highly expressed in mature adipocytes of visceral adipose tissues and is elevated in obese mice. (**A**) Copy numbers of miR-34a in epididymal white adipose tissue (epiWAT), subcutaneous white adipose tissue (scWAT), brown adipose tissue (BAT), liver, and heart of 12-week-old C57BL/6J mice fed with standard chow (STC) (n = 6). (**B**) The mRNA abundance of miR-34a in epiWAT of mice fed with STC or high-fat diet (HFD) for 0, 1, 8, 16, and 32 weeks (n = 6–8). (**C**) The mRNA abundance of miR-34b and miR-34c in the epiWAT of mice on STC or HFD for 16 weeks (n = 5). (**D**) Copy number of miR-34a in mature adipocytes and stromal vascular fraction (SVF) of epiWAT isolated from mice on STC or HFD for 16 weeks (n = 5). (**E**) The mRNA abundance of *Tnfa* in epiWAT of mice on STD or HFD for various periods (n = 6–8). (**F**) Correlation analysis between miR-34a and *Tnfa* levels in the same epiWAT of mice after HFD (n = 35). Correlation was assessed by nonparametric Spearman's test (r = 0.8095, P < 0.001). (**G** and **H**) The mRNA abundance of miR-34a in mature adipocytes treated with vehicle, recombinant TNF-α protein (**G**), or palmitic acid (**H**) for 24 hours (n = 4). Data represent mean ± SEM. Differences between groups were determined by ANOVA (**B**–**E**, **G**, and **H**); *P < 0.05, **P < 0.01, ***P < 0.001. Copy numbers of miR-34a were calculated based on a standard curve generated using a synthetic lin-4. Relative levels of miR-34a, miR-34b, and miR-34c were normalized to sno202, and *Tnfa* mRNA levels were normalized to *18S* RNA abundance.

M2 in response to changing environment (8). The lean adipose tissue is dominated by the M2 macrophage population, which plays a key role in maintaining the proper functioning and homeostasis of the tissue through phagocytosis of dead adipocytes and secretion of antiinflammatory cytokines and other regulatory factors for angiogenesis, adipogenesis, and adaptive thermogenesis (9). However, during the progression of obesity, ATMs undergo a phenotypic switch from the antiinflammatory M2 toward the proinflammatory M1, which produce proinflammatory factors to exacerbate metainflammation and insulin resistance (8, 9). Mice with disruption of PPARγ in myeloid cells had impaired alternative macrophage activation and were prone to diet-induced insulin resistance, whereas forced expression of macrophage PPARδ/β by Th2 cytokines induces polarization of M2 macrophages and enhances insulin sensitivity (10, 11). Previous studies have identified a number of type 2 cytokines (IL-4 and IL-13) produced from eosinophils, $CD4^+$ T cells, or natural killer cells that are important for maintenance of M2 polarization of ATMs (12–14). However, how lipid-loaded hypertrophic adipocytes send signals to trigger infiltration and alter polarization of ATMs in obesity remains poorly understood.

MicroRNAs (miRNAs) are endogenous small noncoding RNAs that regulate gene expression post-transcriptionally by directly binding to the 3′-untranslated region (3′-UTR) of target mRNAs (15, 16). MiRNAs play important roles in a plethora of physiological processes (17), and their dysregulation has been implicated in the pathogenesis of various diseases, including obesity, diabetes, and diabetic complications (18). In particular, numerous miRNAs are present in adipose tissues, actively participating in the regulation of adipogenesis, adipokine secretion, inflammation, and intercellular communications in the local tissues (19). Furthermore, a subset of miRNAs can be packaged into adipose-derived microvesicles and delivered into the bloodstream, acting as hormone-like molecules to facilitate the crosstalk among key metabolic organs (20). Therefore, adipose-derived miRNAs hold great promise as diagnostic biomarkers and therapeutic targets for obesity-related metabolic complications.

In a microarray-based analysis for miRNAs in adipose tissues, we observed a marked upregulation of miR-34a in visceral fat of dietary-obese mice. Coincidently, expression of miR-34a is also increased in adipose tissue of obese humans (21–23), and correlates well with the degree of insulin resistance. To address

the pathophysiological roles of miR-34a in obesity-related adipose inflammation and metabolic dysfunction, we generated adipose tissue–selective miR-34a–KO mice in this study. Interestingly, our results showed that adipose-selective ablation of miR-34a rendered the mice resistant to obesity-induced insulin resistance, glucose intolerance, and hepatosteatosis, all of which were attributed to the alterations of ATMs. Therefore, we further investigated the mechanisms and the clinical implications of miR-34a's mediation of obesity-induced metabolic inflammation via modulation of macrophage biology.

Results

MiR-34a expression in visceral adipose tissue is induced upon dietary stress. To explore the potential involvement of miR-34a in obesity and its associated metabolic complications, we compared the expression of miR-34a in different adipose depots of C57BL/6J mice on standard chow diet (STC) and high-fat diet (HFD). Real-time PCR analysis showed the highest level of miR-34a expression in epididymal white adipose tissue (epiWAT) among the tissues examined (Figure 1A). Furthermore, HFD led to a progressive elevation of miR-34a in epiWAT (Figure 1B). At 16 weeks after HFD, the expression level of miR-34a in epiWAT was more than 3-fold higher than that in STC-fed mice (Figure 1B). In contrast, the other 2 members of the miR-34 family, miR-34b and miR-34c, were not significantly changed after 16 weeks of HFD (Figure 1C). Further analysis for the relative amount of miR-34a in mature adipocytes and the stromal vascular fraction (SVF) from epiWAT showed that the expression of miR-34a was substantially higher in mature adipocytes than in the SVF under both STC and HFD conditions, although HFD-mediated induction of miR-34a occurred in both fractions of epiWAT (Figure 1D). Furthermore, the mRNA level of the inflammatory cytokine *Tnfa,* which was also increased progressively from early to late dietary obesity (Figure 1E), showed a strong positive correlation with miR-34a in obese epiWAT (Figure 1F). Furthermore, treatment of mature adipocytes with recombinant TNF-α protein or palmitic acid led to a dose-dependent induction of miR-34a expression (Figure 1, G and H), suggesting that adipocyte miRNA-34a is an inflammatory responder in obese epiWAT.

Adipose-selective ablation of miR-34a attenuates obesity-induced metabolic dysfunction. To further dissect the biological functions of adipose-resident miR-34a, we generated adipose-selective miR-34a–KO mice by crossing pre–miR-34a–floxed mice with Cre transgenic mice driven by the *aP2* gene promoter on a C57BL/6J background (Supplemental Figure 1, A and B; supplemental material available online with this article; https://doi.org/10.1172/JCI123069DS1). Real-time PCR analysis confirmed that the depletion of miR-34a was restricted in adipose tissues of the KO mice, while its expression in liver and heart was not affected (Supplemental Figure 1C). When the KO mice and their WT littermates were fed with STC, there was no obvious difference in body weight and adiposity between the 2 groups of mice. On the other hand, HFD-induced body weight gain (Figure 2, A and B) and adiposity (Figure 2C) in the miR-34a–KO mice were more prominent than those in WT mice, which was mainly attributed to the expansion of visceral WATs, including epiWAT and retroperitoneal WAT (Figure 2D). These changes in the miR-34a–KO mice were associated with a marked reduction in HFD-induced accumulation of collagen, a major fibrous component of extracellular matrix proteins in adipose tissues (Supplemental Figure 2, A and B). Consistently, HFD-induced expression of several genes involved in adipose fibrosis, including *Col6a1*, *Mmp12*, and *Tgfb1* (24), was significantly decreased in the miR-34a–KO mice as compared with obese WT mice (Supplemental Figure 2, C–E), suggesting that the increased adiposity in HFD-fed miR-34a–KO mice may be attributed to reduced fibrosis, which renders adipose tissues more flexible for expansion.

We next monitored the dynamic changes in glucose and lipid metabolism as well as insulin sensitivity at different time points (0, 4, 8, and 16 weeks) after feeding the 2 groups of mice with HFD. As expected, WT mice on HFD exhibited progressive development of glucose intolerance, hyperinsulinemia, and insulin resistance (Figure 2, E–G). Interestingly, despite increased adiposity, the miR-34a–KO mice were much more glucose tolerant and insulin sensitive than WT littermates at 8 weeks, and these differences became even more obvious at 16 weeks after HFD. Consistently, Western blotting analysis demonstrated that while the insulin-stimulated phosphorylation of Akt (Ser 473) was blunted in epiWAT of obese WT mice, this insulin signaling response was largely preserved in KO mice (Figure 2, H and I).

Mice with adipose-specific deletion of miR-34a displayed significant reductions in serum triglyceride levels after HFD for 8 weeks (Supplemental Figure 3A). Furthermore, while HFD-fed WT mice showed the characteristic signs of nonalcoholic fatty liver disease (including enlarged, paler liver and increased amount of hepatic lipid deposition), these symptoms were significantly attenuated in miR-34a–KO mice (Supplemental Figure 3, B–E). In contrast to these observations, there was no difference in the miR-34a levels in liver between WT and adipose-specific miR-34a–KO mice (Supplemental Figure 3F), indicating that the reduced fatty liver in the KO mice was secondary to local alterations in adipose tissue biology upon miR-34a deletion.

Obesity-evoked macrophage infiltration and polarization toward M1 subtype in adipose tissues are dampened by deletion of miR-34a. We next examined whether the improvements in glucose metabolism and insulin sensitivity in adipose-selective miR-34a–KO mice were associated with alleviation of adipose inflammation. Histological analysis detected the presence of adipose inflammation, typified by macrophage crown-like structures (CLSs) in epiWAT at 8 weeks, and the number of CLSs was almost doubled at 16 weeks after HFD (Figure 3, A and B, and Supplemental Figure 3G). However, no obvious CLSs were observed in HFD-fed adipose-specific miR-34–KO mice. Consistently, FACS analysis showed that HFD-induced elevation in the number of $F4/80^+$ macrophages in the SVF of epiWAT in adipose-specific miR-34–KO mice was significantly lower than that in WT littermates (Figure 3C). In WT mice on HFD for 16 weeks, over 36.5% ± 9.3% of macrophages in epiWAT were classically activated proinflammatory M1 macrophages (defined as $F4/80^+CD11c^+CD206^-$), whereas alternatively activated antiinflammatory M2 macrophages ($F4/80^+CD11c^-CD206^+$) only accounted for 32.4% ± 10.5% (Figure 3D). Notably, the adipose-resident M1 macrophages in the HFD-fed KO mice were markedly reduced to 21.2% ± 4.5%, which was accompanied by a significant

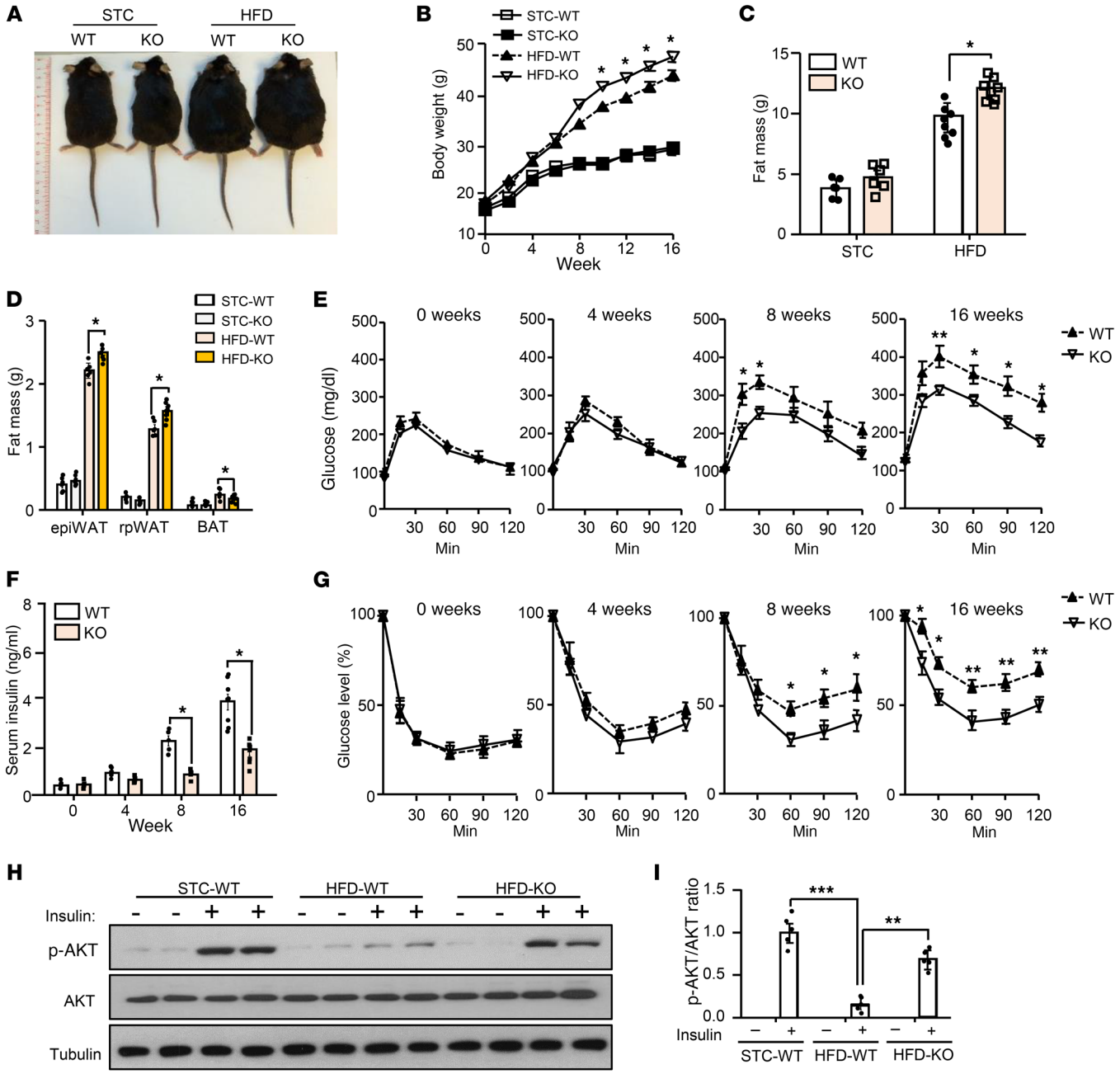

Figure 2. Adipose tissue–specific ablation of miR-34a protects mice from obesity-induced glucose intolerance and insulin resistance. (**A**) Representative photos of adipose-specific miR-34a–KO mice and their WT miR-34a$^{fl/fl}$ littermates fed with either STC or HFD for 16 weeks. (**B**) Dynamic changes in body weight of WT and KO mice during 16 weeks of STC or HFD feeding (n = 6–8). (**C** and **D**) Fat mass of whole body (**C**) and individual tissues (**D**) (n = 6–8). (**E**) Glucose tolerance test after mice were fed with HFD for 0, 4, 8, and 16 weeks (n = 6–8). (**F**) Serum concentrations of fed insulin in mice on HFD for 0, 4, 8, and 16 weeks (n = 6–8). (**G**) Insulin tolerance test after mice were fed with HFD for 0, 4, 8, and 16 weeks (n = 6–8). (**H** and **I**) The KO mice or WT littermates on STC or HFD for 16 weeks were injected intraperitoneally with insulin (2 IU/kg body weight) for 10 minutes. (**H**) Immunoblot analyses of epiWAT samples using antibodies against phospho-AKT (p-AKT-S473), total AKT, and tubulin. (**I**) Densitometry analysis for the p-AKT/AKT ratio (n = 4–5). Data represent mean ± SEM. Differences between WT and KO mice were determined by ANOVA (**B**–**G** and **I**); $^*P < 0.05$, $^{**}P < 0.01$, $^{***}P < 0.001$.

elevation of the M2 macrophages (69.3% ± 2.1%). In line with this finding, epiWAT from dietary-obese KO mice expressed a much lower protein level of the M1 macrophage marker inducible NO synthase (iNOS), along with a higher abundance of the M2 macrophage marker arginase 1 (Arg1) (Figure 3, E and F). Likewise, compared with the obese WT mice, the KO mice exhibited obvious reductions in mRNA expression of the M1 macrophage–related genes (*Tnfa*, *Il6*, *Il1b*, *iNos*, and *Mcp1*), but significant upregulation of M2 macrophage–related genes (*Fizz1*, *Ym1*, *Arg1*, and *Il10*) (Figure 3G). Similarly, HFD also increased miR-34a level in subcutaneous fat (Supplemental Figure 3H), accompanied by increased expression level of the inflammatory cytokines, including *Tnfa*, *Il6*, and *iNos* (Supplemental Figure 3, I–K). Adipose miR-34a ablation significantly decreased

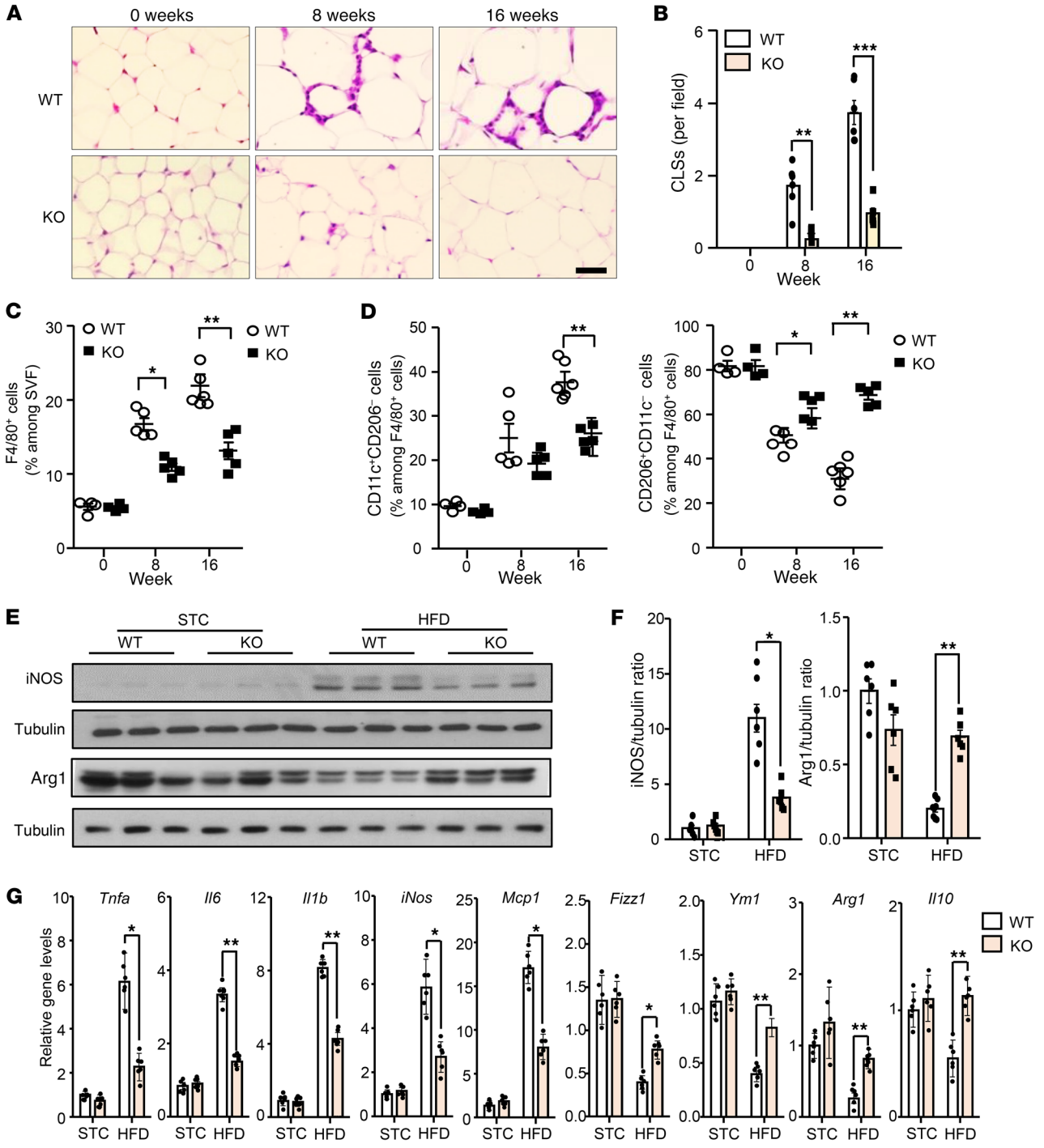

Figure 3. Adipose miR-34a modulates infiltration and polarization of macrophages in mice with dietary obesity. (**A** and **B**) Representative images of immunohistological staining of F4/80 (**A**) and quantification of crown-like structures (CLSs; **B**) in epiWAT of WT or KO mice on HFD for 0, 8, and 16 weeks (n = 6). Scale bar: 40 μm. (**C** and **D**) Cells isolated from SVFs of epiWAT in KO and WT mice fed with HFD for 0, 8, and 16 weeks were subjected to flow cytometry analysis for percentage of F4/80$^+$ total macrophages (**C**), M1 (CD11c$^+$CD206$^-$), and M2 (CD206$^+$CD11c$^-$) within the macrophage population (**D**) (n = 4–6). (**E** and **F**) Immunoblot analysis for the expression of iNOS and arginase 1 (Arg1) in epiWAT of mice on STC or HFD for 16 weeks (**E**), and densitometric analysis for their abundance relative to tubulin (**F**) (n = 6–8). (**G**) Real-time PCR analysis for the mRNA levels of the M1 and M2 markers in epiWAT of mice on STD or HFD 16 weeks (n = 6). Data represent mean values ± SEM. Differences between groups were determined by ANOVA (**B**–**D**, **F**, and **G**); $^*P < 0.05$, $^{**}P < 0.01$, $^{***}P < 0.001$. Gene levels were normalized to *18S* RNA abundance.

HFD-induced inflammatory responses in subcutaneous adipose tissues, and also markedly blunted HFD-induced elevation in serum levels of several inflammatory factors (TNF-α, IL-6, IL-1β, and MCP-1) and FGF21 (Supplemental Figure 3, L–P). In contrast, HFD-induced reduction in circulating levels of adiponectin, an adipokine with insulin-sensitizing and antiinflammatory properties, was largely reversed in the miR-34a–KO mice (Supplemental Figure 3Q).

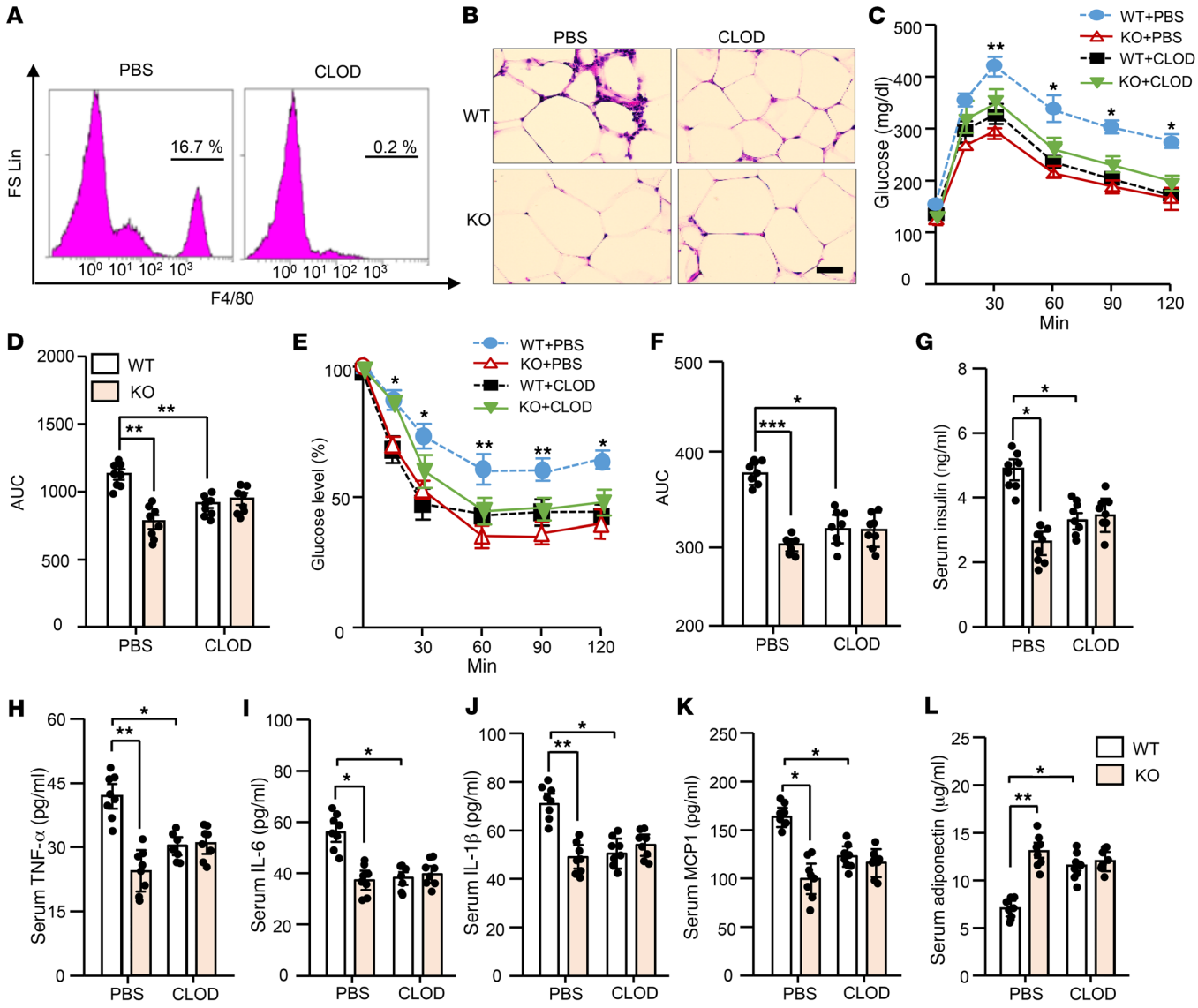

Figure 4. The metabolic benefits of adipose-selective miR-34a deficiency are mediated by macrophages. Male adipose-specific miR-34a–KO mice or WT controls on HFD for 12 weeks were intraperitoneally injected with PBS-liposomes or clodronate-conjugated liposomes (CLOD-liposomes) for 4 weeks. (**A**) Representative flow cytometry dot plots showing F4/80$^+$ total macrophages in SVFs of epiWAT from HFD-fed WT mice injected with PBS- or CLOD-liposomes for 4 weeks. (**B**) Representative images of immunohistological staining of F4/80 in epiWAT from WT and KO mice treated with PBS- or CLOD-liposomes. Scale bar: 40 μm. (**C**) Glucose tolerance test of HFD-fed WT and KO mice treated with PBS- or CLOD-liposomes (n = 8; $^*P < 0.05$, $^{**}P < 0.01$ compared with KO+PBS). (**D**) Area under the curve (AUC) of glucose tolerance test (n = 8). (**E**) Insulin tolerance test of mice (n = 8; $^*P < 0.05$, $^{**}P < 0.01$ compared with KO+PBS). (**F**) AUC of insulin tolerance test (n = 8). (**G**–**L**) Serum levels of insulin (**G**), TNF-α (**H**), IL-6 (**I**), IL-1β (**J**), MCP-1 (**K**), and adiponectin (**L**) determined with ELISA (n = 8). Data represent mean ± SEM. Differences were determined by ANOVA (**C**–**L**); $^*P < 0.05$, $^{**}P < 0.01$, $^{***}P < 0.001$.

Similar to the changes observed in male mice, miR-34a expression in epiWAT of female mice was also increased approximately 2-fold after feeding with HFD for 12 weeks (Supplemental Figure 4A). Likewise, HFD-fed female mice with ablation of adipose miR-34a exhibited a modest gain in body weight and total fat mass (Supplemental Figure 4, B and C), but significant alleviations of glucose intolerance, hyperinsulinemia, and insulin resistance, compared with WT controls (Supplemental Figure 4, D–H). These metabolic changes in HFD-fed miR-34a–KO female mice were also accompanied by a reduced number of F4/80$^+$ total macrophages, decreased percentage of F4/80$^+$CD11c$^+$ M1 macrophages, but increased composition of F4/80$^+$CD206$^+$ M2 macrophages in epiWAT (Supplemental Figure 4, I and J). Likewise, adipose-specific ablation of miR-34a also led to obvious reductions in the mRNA expression of M1 macrophage–related genes (*Tnfa*, *Il6*, *Il1b*, *iNos*, and *Mcp1*) but significant upregulation of M2 macrophage–related genes (*Fizz1*, *Ym1*, *Arg1*, and *Il10*) in female mice on HFD (Supplemental Figure 4K).

MiR-34a regulates monocyte recruitment and M2 macrophage proliferation independently of Th2 cytokines. In mice on either STC or HFD, adipose-selective depletion of miR-34a had no effect on expression of several type 2 cytokines, including *Il4*, *Il5*, and *Il13* (Supplemental Figure 5A), which are well-known regulators of M2 macrophages (12). We next investigated the effect of adipose miR-34a KO on eosinophils and group 2

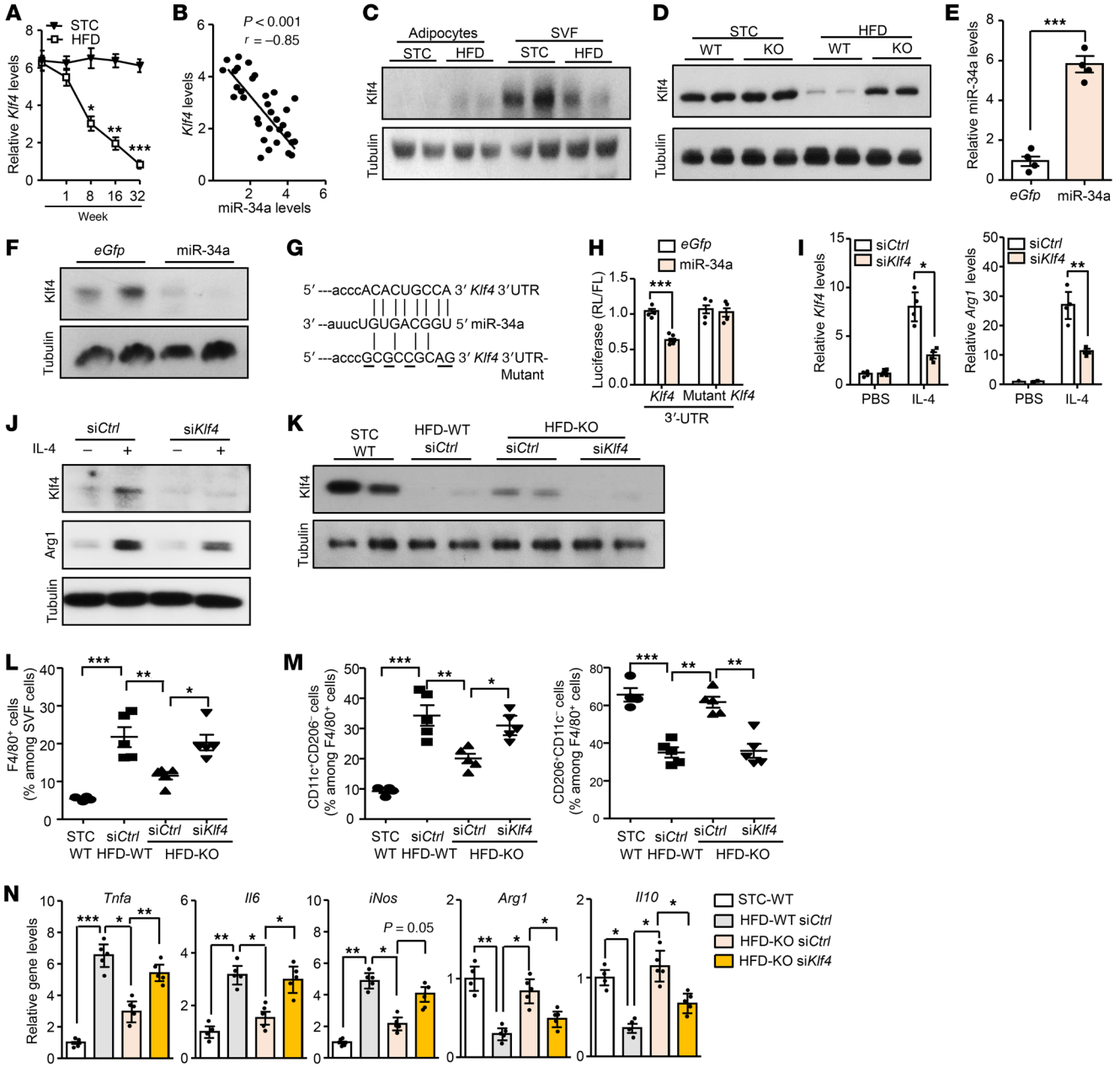

Figure 5. MiR-34a modulates inflammation and macrophage polarization by targeting *Klf4*. (**A**) The mRNA abundance of *Klf4* in epiWAT of mice (n = 6–8). (**B**) Correlative analysis between the mRNA abundance of miR-34a and *Klf4* levels (n = 35). Correlation was assessed by nonparametric Spearman's test. (**C**) The protein levels of Klf4 in mature adipocytes and SVF of epiWAT isolated from mice on STC or HFD for 16 weeks. (**D**) Immunoblot analysis for Klf4 protein in SVF. (**E** and **F**) Analysis of miR-34a levels (**E**) and Klf4 protein levels (**F**) in bone marrow derived macrophages (BMDMs) infected with lentivirus encoding *eGfp* or miR-34a. (n = 4). (**G** and **H**) A schematic diagram showing the construction of the luciferase reporter vectors (**G**), and luciferase assays were performed in HEK293 cells (**H**, n = 4). Data are presented as ratio of Renilla luciferase (RL) to firefly luciferase (FL) activity. (**I** and **J**) BMDMs were infected with lentivirus for 24 hours, followed by stimulation with IL-4 (10 ng/ml) for 24 hours. Analysis of gene expression of *Klf4* and *Arg1* (**I**) and protein levels of Klf4 and Arg1 (**J**) (n = 4). (**K**–**N**) KO and WT littermates on HFD for 14 weeks were locally injected with lentivirus expressing siRNA against Klf4 (si*Klf4*) or scramble control (si*Ctrl*) in epiWAT for 2 weeks. (**K**) Immunoblot analysis for KLF4 protein in SVFs. (**L** and **M**) Flow cytometric quantification for percentage of total macrophages (**L**), M1 and M2 macrophages in SVFs (**M**, n = 4–5). (**N**) The mRNA abundance of M1 macrophage–associated genes in epiWAT (n = 4–5). Data represent mean ± SEM. Differences were determined by ANOVA (**A**, **H**, **I**, and **L**–**N**) or Student's t test (**E**); $^*P < 0.05$, $^{**}P < 0.01$, $^{***}P < 0.001$. MiR-34a abundance was normalized to sno202 level, and other gene levels were normalized to *18S* RNA abundance.

innate lymphoid cells (ILC2s), which have been reported to modulate adipose remodeling under obese conditions (12, 25). Flow cytometry analysis showed that the numbers of CD11b$^+$SiglecF$^+$SSC^{hi} eosinophils and CD25$^+$IL33R$^+$SSC^{hi} ILC2s were significantly decreased in epiWAT after HFD treatment in both KO and WT mice, whereas there was no obvious difference between KO and WT mice on either STC or HFD (Supplemental Figure 5, B and C). Notably, adipose-selective ablation of

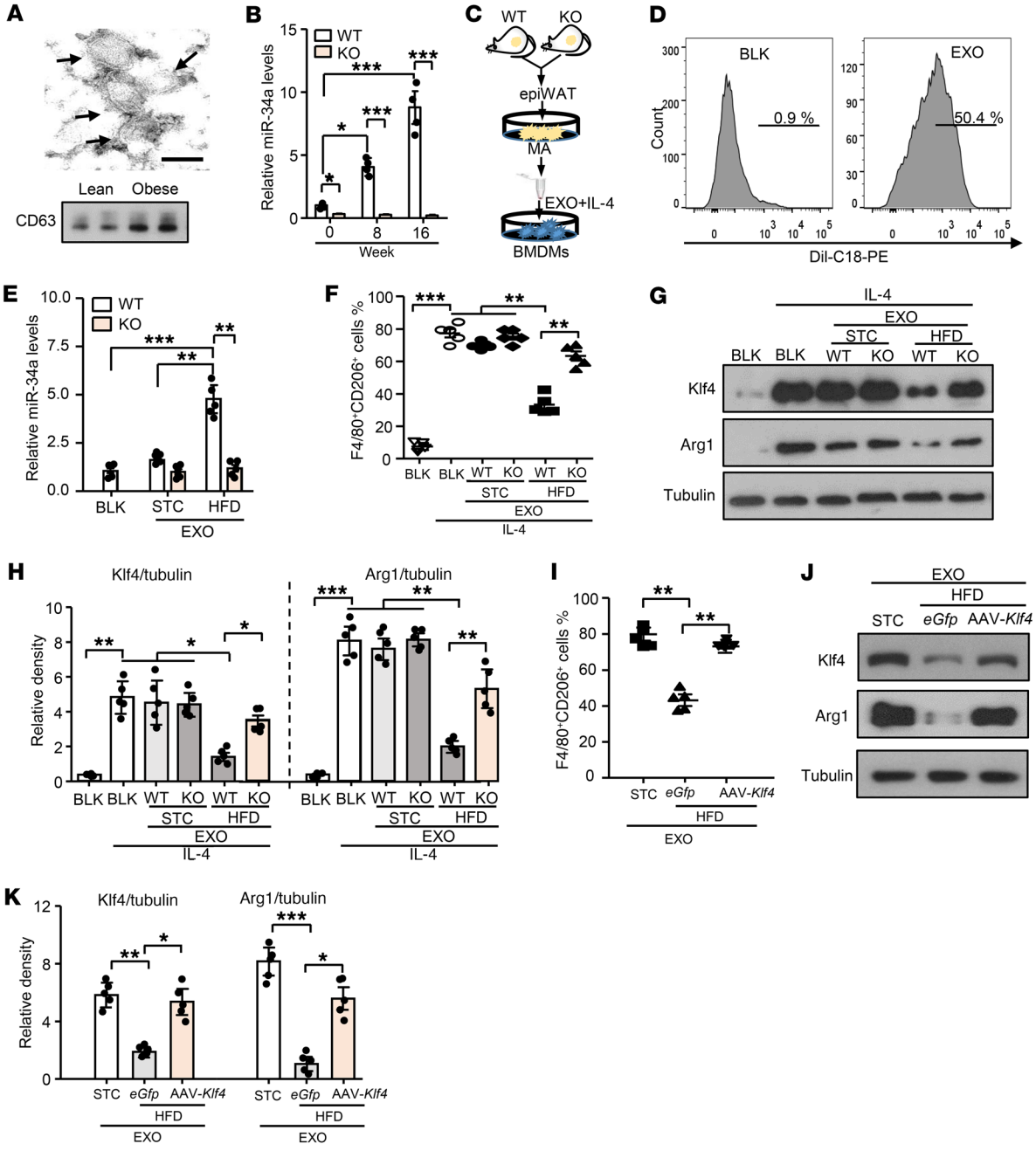

Figure 6. Exosomes secreted from mature adipocytes transport miR-34a into macrophages to suppress M2 polarization via downregulation of KLF4. (**A**) Electron microscopy (top panel) and Western blot analysis (bottom panel) of exosomes (EXO) secreted by adipocytes (scale bar: 100 nm). (**B**) Mature adipocytes (MA) in epiWAT were isolated from miR-34a KO or their WT littermates fed with HFD and cultured in 1 ml FBS-free DMEM for 48 hours. Analysis of miR-34a levels in isolated exosomes from conditional medium (n = 6–8). (**C**–**E**) Isolated exosome was prestained with DiI-C18 and applied to IL-4–treated BMDMs for 24 hours. Schematic depiction of the experiment (**C**). Flow cytometry analysis for the percentage of DiI-C18–positive BMDMs (**D**). Abundance of miR-34a in BMDMs stimulated with exosomes from KO mice and WT littermates (**E**). Blank DMEM (BLK) was used as control (n = 5). (**F**–**H**) BMDMs were pretreated without or with exosomes secreted from KO mice and WT littermates, followed by treatment without or with IL-4 for 24 hours. Percentage of M2 macrophages as determined by flow cytometry (**F**). Immunoblot analyses of Klf4 and Arg1 protein levels (**G**) and densitometry analysis (**H**) (n = 5). (**I**–**K**) BMDMs were infected with 1.5 × 10^6 viral particles of adeno-associated virus (AAV), followed by treatment with exosomes derived from mice on HFD or STC for 16 weeks in the presence of IL-4 for another 24 hours. Percentage of M2 macrophages as determined by flow cytometry (**I**). Immunoblot analyses of Klf4 and Arg1 protein levels (**J**), and densitometry analysis (**K**) (n = 5). Data represent mean ± SEM. Differences were determined by ANOVA (**B**, **E**, **F**, **H**, **I**, and **K**); *P < 0.05, **P < 0.01, ***P < 0.001. MiR-34a levels were normalized to sno202 for all experiments, and other gene levels were normalized to *18S* RNA abundance.

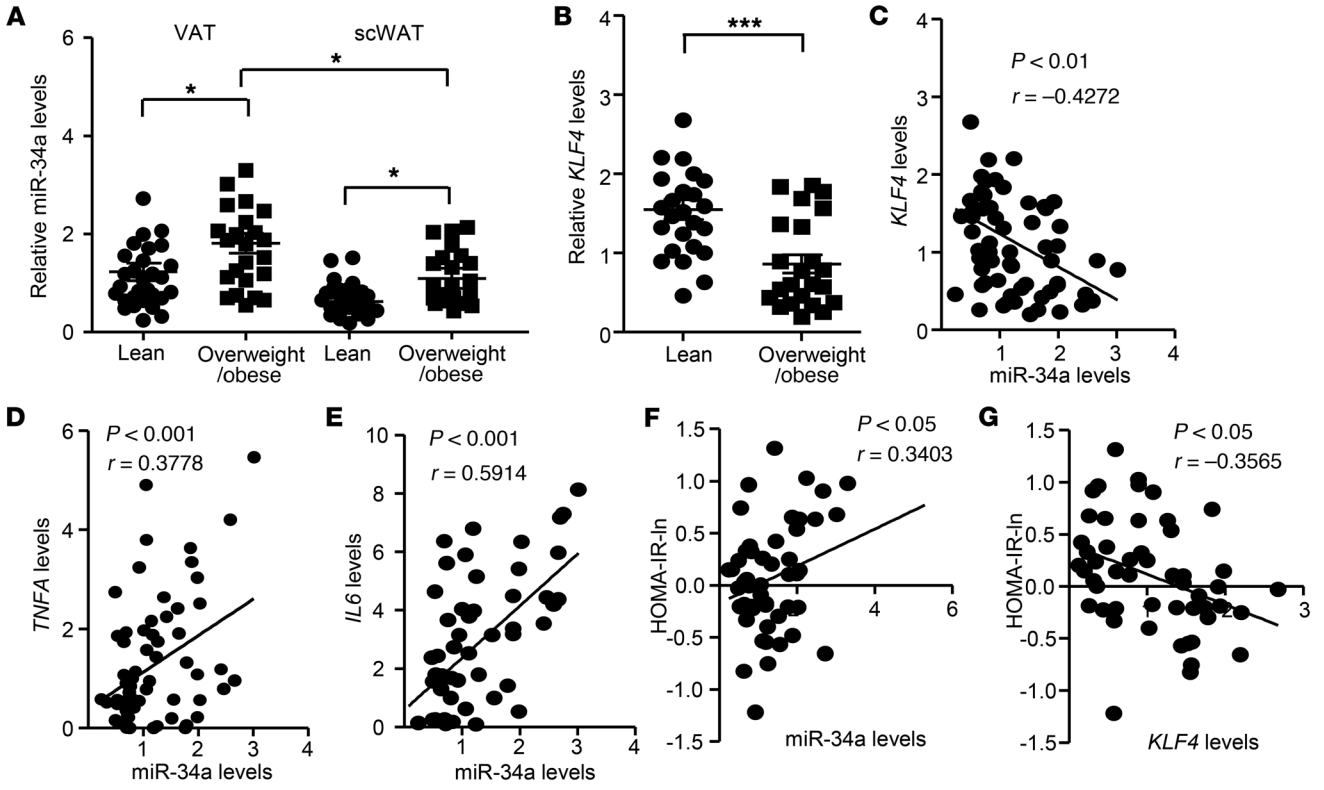

Figure 7. Dysregulated miR-34a/KLF4 axis in adipose tissues is associated with inflammation and insulin resistance in overweight/obese Chinese subjects. (**A**) Real-time PCR analysis for the expression levels of miR-34a in visceral adipose tissue (VAT) and subcutaneous white adipose tissue (scWAT) from 29 lean and 24 overweight/obese individuals undergoing elective abdominal surgery for benign, noninfective gynecological conditions. (**B**) Gene expression of *Klf4*. (**C**) Correlation between miR-34a and *KLF4* levels in visceral fat of these study subjects. (**D** and **E**) The association between miR-34a and the mRNA abundance of *TNFA* (**D**) and *IL6* (**E**) in visceral fat. (**F** and **G**) Correlation between the insulin resistance index (HOMA-IR) and the expression level of miR-34a (**F**) or *KLF4* (**G**) in the visceral fat. Data represent mean ± SEM. Differences were determined by ANOVA (**A**) or Student's *t* test (**B**), and correlation was assessed by nonparametric Spearman's test (**C**–**G**); $^{*}P < 0.05$, $^{***}P < 0.001$. MiR-34a expression was normalized to sno202 levels, and gene abundance of *Klf4*, *TNFA*, and *IL6* were normalized to *18S* RNA abundance.

miR-34a has no effect on the expression and phosphorylation of STAT6 (Supplemental Figure 5D), a key transcriptional factor that induces macrophage polarization to M2 phenotypes (26, 27). Taken together, these data suggest that Th2 cytokines, eosinophils, or ILC2s are not the direct targets of adipose miR-34a, and STAT6 is not involved in miR-34a–mediated macrophage polarization.

To investigate how miR-34a mediates obesity-induced changes in the number and phenotypes of adipose-resident macrophages, we first evaluated the impact of miR-34a deficiency on recruitment of circulating monocytes into adipose tissues by tail vein injection of monocytes labeled with the fluorescent dye PKH26 into the miR-34a–KO mice or WT littermates, followed by flow cytometry analysis. In line with previous reports (28, 29), HFD led to a marked increase in the infiltration of circulating monocytes into epiWAT of WT mice compared with lean controls (Supplemental Figure 6A), and the newly recruited monocytes were mostly converted to $PKH26^{+}CD11c^{+}$ M1 macrophages (Supplemental Figure 6, B and C). Adipose miR-34a deficiency significantly decreased the recruitment of circulating monocytes, accompanied by reduced conversion into $PKH26^{+}CD11c^{+}$ M1 macrophages, but increased conversion to $PKH26^{+}CD206^{+}$ M2 macrophages.

As local self-renewal also contributes to the maintenance of tissue-resident macrophages, we next interrogated the roles of miR-34a in macrophage proliferation in epiWAT by subcutaneous injection with the thymidine analog 5-ethynyl-2′-deoxyuridine (EdU) to label the dividing cells, followed by quantification of the EdU^{+} proliferating macrophages with flow cytometry. The percentage of proliferating $EdU^{+}F4/80^{+}$ macrophages was comparable between the miR-34a–KO mice and WT littermates on STC (Supplemental Figure 6D). HFD modestly increased the proliferation of macrophages, which was mainly attributed to increased proliferation of $EdU^{+}F4/80^{+}CD206^{+}$ M2 macrophages but not $EdU^{+}F4/80^{+}CD11c^{+}$ M1 macrophages (Supplemental Figure 6, D–F). Intriguingly, adipose miR-34a ablation selectively augmented the proliferation of M2 macrophages in epiWAT of HFD-fed mice. These data collectively suggest that the reduced number of total macrophages and increased M2/M1 ratio in adipose tissues of HFD-fed miR-34a–KO mice are attributable to decreased infiltration of circulating monocytes, increased conversion of infiltrated monocytes into M2 phenotypes, and increased local proliferation of M2 macrophages.

Modulation of whole-body metabolism by adipose miR-34a requires macrophages. Given the striking effects of miR-34a on infiltration and polarization of macrophages, we next investigated whether the metabolically healthy phenotypes in adipose-selective

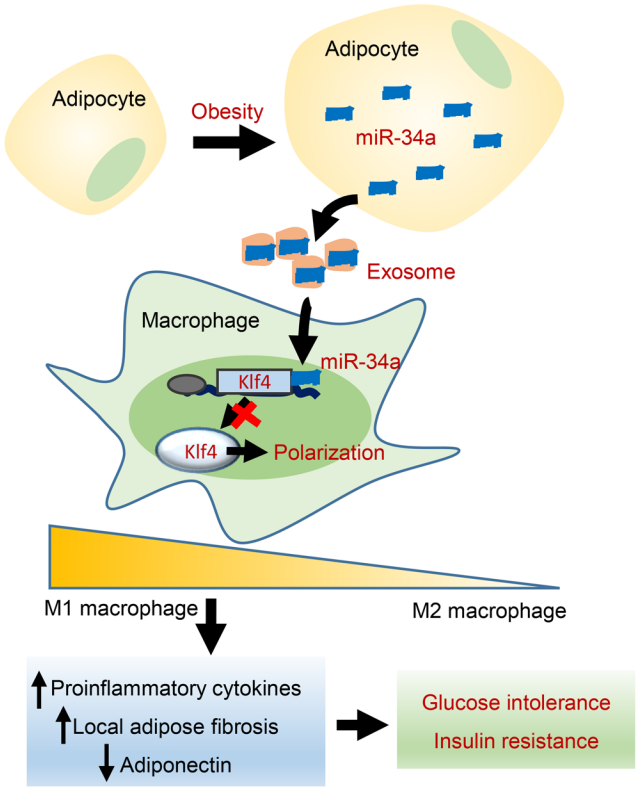

Figure 8. Schematic summary of the role of adipocyte-secreted exosomal miR-34a in obesity-induced alterations in macrophage polarization, adipose inflammation, and insulin resistance. Hypertrophic adipocytes in obese adipose tissue release exosomes, which carry miR-34a to adipose-resident macrophages, where it shifts macrophage polarization from M2 to M1 by downregulation of Klf4, thereby leading to induction of proinflammatory cytokines and local fibrosis and downregulation of adiponectin, thereby leading to systemic insulin resistance and glucose intolerance.

miR-34a–KO mice depend on the presence of macrophages. To this end, both adipose-specific miR-34a–KO mice and WT littermates were intraperitoneally injected with clodronate-conjugated liposomes (CLOD-liposomes) to deplete macrophages (30), or PBS-liposomes as vehicle control. The successful depletion of adipose-resident macrophages by CLOD-liposomes was verified by both flow cytometry (Figure 4A) and histological analysis showing a remarkably reduced number of CLSs in epiWAT in HFD-fed obese mice (Figure 4B).

Consistent with previous reports (31, 32), macrophage depletion with CLOD-liposomes obviously alleviated glucose intolerance and insulin resistance in HFD-fed obese WT mice, and abrogated the differences of these metabolic parameters between miR-34a–KO mice and WT mice (Figure 4, C–F). Furthermore, macrophage depletion also led to a significant reduction in serum levels of insulin and several proinflammatory factors (TNF-α, IL-6, IL-1β, and MCP-1) but elevated circulating adiponectin in obese WT mice (Figure 4, G–L), suggesting that macrophages are an important contributor to obesity-related systemic inflammation and hypoadiponectinemia. Notably, the differences in these circulating factors between miR-34a–KO mice and WT littermates became indistinguishable after macrophage depletion. Taken together, these data support macrophages as an important mediator for adipose miR-34a–induced systemic inflammation, insulin resistance, and glucose dysregulation in obesity.

MiR-34a controls macrophage polarization by targeting Krüppel-like factor 4. To search for the potential transcriptional factors by which miR-34a regulates adipose macrophage infiltration and polarization, we adopted mirSVR and PhastCons analysis to predict possible targets of miR-34a that regulate macrophage biology (33). As shown in Supplemental Table 1, the predicted binding between miR-34a and the 3′-UTR of the Krüppel-like factor 4 (*Klf4*) gene exhibited the highest mirSVR and PhastCons scores in comparison with other transcription factors involved in macrophage function and polarization. Indeed, in contrast to the elevated levels of miR-34a, the mRNA abundance of *Klf4* in epiWAT was progressively decreased after feeding of the mice with HFD (Figure 5A). Correlation analysis revealed a strong negative association between miR-34a and mRNA expression of *Klf4* (Figure 5B). Further immunoblot analysis showed that expression of Klf4 in the SVF was substantially higher than in mature adipocytes under STC condition, and was obviously decreased after HFD for 16 weeks (Figure 5C). Notably, the HFD-induced reduction of Klf4 in SVF of epiWAT was largely reversed in adipose-specific miR-34a–KO mice (Figure 5D). Conversely, lentivirus-mediated overexpression of miR-34a (Figure 5E) in bone marrow–derived macrophages greatly suppressed the protein expression of Klf4 (Figure 5F).

To verify that *Klf4* is indeed a direct target of miR-34a, the putative miR-34a–binding sequence at the 3′-UTR of the *Klf4* gene was subcloned to a luciferase reporter vector (Figure 5G). Ectopic expression of miR-34a significantly reduced the luciferase activity in HEK293 cells transfected with the reporter vector containing the *Klf4* 3′-UTR sequence, whereas such an effect of miR-34a was abolished when the binding sequence was mutated (Figure 5H).

Klf4 is crucial for maintaining adipose M2 macrophage phenotype in miR-34a–KO mice. To address whether the increase in M2 macrophages in adipose tissues of miR-34a–KO mice is attributable to elevated Klf4, we generated lentivirus expressing siRNA targeting *Klf4* (si*Klf4*) or scramble siRNA (si*Ctrl*) (Figure 5, I and J) and administrated these viruses into epiWAT of HFD-fed KO mice by local injection. At 2 weeks after injection of lentiviruses expressing si*Klf4*, the expression of Klf4 in epiWAT of HFD-fed KO mice was reduced to a level similar to that in HFD-fed WT mice (Figure 5K). Notably, downregulation of *Klf4* led to significant increases in the counts of total macrophages (Figure 5L) and M1 macrophages (Figure 5M) in epiWAT of HFD-fed KO mice compared with those treated with lentivirus expressing si*Ctrl*. Moreover, flow cytometry analysis showed that knockdown of *Klf4* significantly reduced the composition of adipose-resident M2 macrophages in epiWAT of HFD-fed KO mice to a level comparable to that in HFD-fed WT mice (Figure 5M). Similarly, the reduced expression of M1 macrophage–associated proinflammatory factors (*Tnfa*, *Il6*, *iNos*) and increased abundance of M2 macrophage–related antiinflammatory markers (*Arg1*, *Il10*) in epiWAT of HFD-fed miR-34a–KO mice were reversed by the lentivirus-mediated knockdown of *Klf4* (Figure 5N).

To further interrogate whether downregulated expression of Klf4 is a contributor to obesity-induced adipose inflammation, HFD-fed mice were locally injected with adeno-associated virus overexpressing either *Klf4* or *eGfp* (as control) into epiWAT. The

successful overexpression of *Klf4* was verified by fluorescence staining (Supplemental Figure 7A) and immunoblot analysis in vivo (Supplemental Figure 7B). Forced expression of Klf4 in epiWAT suppressed HFD-induced formation of CLSs (Supplemental Figure 7B), accompanied by a decreased percentage of total macrophages and M1 macrophages, but an increased percentage of M2 macrophages (Supplemental Figure 7, C and D). Meanwhile, overexpression of *Klf4* reduced expression of M1 macrophage–associated proinflammatory markers and augmented expression of the antiinflammatory genes in comparison with HFD-fed mice treated with adeno-associated virus expressing *eGfp* controls (Supplemental Figure 7E). Taken together, these findings support the notion that elevated miR-34a induces adipose inflammation at least in part by downregulation of Klf4, thereby leading to compromised polarization of M2 macrophages.

Adipocyte-secreted exosomal MiR-34a acts in a paracrine manner to suppress polarization of M2 macrophages. Given that miR-34a is predominantly expressed in mature adipocytes but exerts profound effects on ATMs, we next investigated whether it is secreted from adipocytes via exosomes, which can transport microRNAs to mediate intercellular communications (34). To this end, we isolated the exosomes from the conditional medium of mature adipocytes in visceral adipose tissues of C57BL/6J mice on HFD using ultracentrifugation methods (35). Electron microscopic examination and Western blot analysis revealed that isolated particles contained abundant extracellular vesicles with a diameter of 30–100 nm, and expressed a high level of CD63, a protein marker enriched in the exosomes (Figure 6A and ref. 36). Notably, real-time PCR analysis demonstrated that HFD led to a progressive elevation of miR-34a in the exosomes isolated from adipocytes of WT mice, but not from KO mice (Figure 6B). Therefore, we next stained the exosomes with the fluorescent dye Dil-C18, and treated bone marrow–derived macrophages with the Dil-C18–labeled exosomes (Figure 6C). After a 24-hour incubation with Dil-C18–stained exosomes, 52.2% ± 6.1% of macrophages were stained with Dil-C18 (Figure 6D). Real-time PCR demonstrated that macrophagic miR-34a level was significantly increased after stimulation with exosomes isolated from HFD-fed WT mice (Figure 6E), suggesting that adipocyte-secreted exosomal miR-34a can be transported to macrophages.

To test whether adipocyte-secreted exosomal miR-34a acts in a paracrine manner to modulate macrophage polarization, bone marrow–derived macrophages were incubated with the exosomes isolated from the conditional medium of primary mature adipocytes for 24 hours, followed by induction of M2 polarization with IL-4 for another 24 hours. Flow cytometry analysis showed that IL-4 induced polarization of 78.32% ± 8.50% of cells into F4/80$^+$CD206$^+$ M2 macrophages. Incubation with the exosomes isolated from WT mice on STC caused a modest reduction of IL-4–induced M2 polarization to 69.43% ± 2.61%, whereas incubation with the exosomes from HFD-fed WT mice further decreased the percentage of IL-4–induced M2 macrophages to 40.32% ± 4.51% ($P < 0.01$) (Figure 6F). On the other hand, the inhibitory effects of the exosomes isolated from adipocytes of miR-34a–KO mice on IL-4–induced M2 polarization were markedly attenuated in comparison with WT mice under both STC and HFD. Likewise, Western blot analysis showed that IL-4–induced expressions of Klf4 and Arg1 were significantly reduced by incubation with adipocyte-secreted exosomes of HFD-fed WT mice, whereas such inhibitory effects of the exosomes were largely reversed by miR-34a depletion (Figure 6, G and H). Consistently, the suppressive effects of the adipocyte-secreted exosomes on IL-4–induced elevation of F4/80$^+$CD206$^+$ M2 macrophages and expression of Klf4 and Arg1 were significantly reversed by cotreatment with the miR-34a sponges (Supplemental Figure 8, A–C), suggesting that miR-34a is a key exosomal component responsible for the suppressive effect on polarization of M2 macrophages.

To further address whether adipocyte-secreted exosomal miR-34a inhibits IL-4–induced M2 macrophage polarization by targeting Klf4, bone marrow–derived macrophages were infected with adeno-associated virus overexpressing *Klf4* or *eGfp* (as control) for 24 hours, followed by incubation with the adipocyte-secreted exosomes isolated from HFD-fed WT mice for 24 hours and induction of M2 polarization with IL-4 for another 24 hours. Flow cytometry analysis showed that ectopic expression of Klf4 was sufficient to counteract the exosome-mediated suppression of IL-4–induced polarization of macrophages to M2 phenotypes (Figure 6, I–K), further confirming that Klf4 is an obligatory target of adipocyte-secreted exosomal miR-34a in suppression of M2 polarization.

To further confirm that adipocyte-secreted miR-34a controls polarization of adipose-resident macrophages, we also generated adipocyte-specific miR-34a–KO mice by crossing pre–miR-34a–floxed mice with transgenic mice expressing Cre recombinase under the control of the mouse adiponectin (*Adipoq*) promoter/enhancer regions (named as Adipoq-miR34aKO mice). As expected, depletion of miR-34a was observed only in adipose tissues, not in other organs of Adipoq-miR34aKO mice (data not shown). Notably, HFD-induced elevation of miR-34a in epiWAT was completely abrogated in Adipoq-miR34aKO mice, suggesting that mature adipocytes are the major source for adipose expression of miR-34a (Supplemental Figure 9A). Similarly to the miR-34a–KO mice generated with the *aP2*-Cre driver, Adipoq-miR34aKO mice on HFD also exhibited a modest increase in body weight and fat mass (Supplemental Figure 9, B and C), but significant alleviation of glucose intolerance, hyperinsulinemia, and insulin resistance (Supplemental Figure 9, D–H). Furthermore, marked reductions in HFD-induced formation of CLSs, accumulation of total F4/80$^+$ macrophages, and composition of F4/80$^+$CD11c$^+$ M1 macrophages, but significant increases in the percentage of F4/80$^+$CD206$^+$ M2 macrophages and in Klf4 expression, were also observed in epiWAT of HFD-fed Adipoq-miR34aKO mice compared with those in WT littermates (Supplemental Figure 9, I–N). These changes in Adipoq-miR34aKO mice were accompanied by downregulation of the M1 macrophage–related genes (*Tnfa*, *Il6*, *iNos*, and *Mcp1*), but significant upregulation of M2 macrophage–related genes (*Fizz1*, *Ym1*, *Arg1*, and *Il10*) (Supplemental Figure 9M), reduced serum levels of proinflammatory factors (TNF-α, IL-6, IL-1β, and MCP-1), but elevated circulating adiponectin (Supplemental Figure 9, O–T).

The altered miR-34a/KLF4 axis in visceral fat is closely associated with insulin resistance in obese subjects. To evaluate the clinical relevance of our findings in animal models, both visceral and subcutaneous adipose tissues were collected from 24 overweight/obese (BMI ≥ 23) subjects and 29 age-matched lean female subjects (BMI < 23) undergoing elective abdominal surgery for benign, noninfective gynecological conditions at Queen Mary Hospital, University of Hong Kong (Supplemental Table 2). As expected,

overweight/obese subjects exhibited more adverse glucose and lipid profiles and were more insulin resistant than age-matched lean individuals. Consistent with our animal data, the expression of miR-34a in both adipose depots of overweight/obese individuals was significantly increased compared with that in lean subjects (Figure 7A). Nevertheless, the magnitude of overweight/obesity–associated miR-34a increase was substantially higher in visceral fat than in subcutaneous fat ($P < 0.05$). The expression level of *KLF4* in visceral fat of overweight/obese individuals was significantly reduced by over 40% in comparison with lean subjects (Figure 7B). Furthermore, the expression level of miR-34a correlated negatively with *KLF4* ($r = -0.4272$, $P < 0.01$; Figure 7C) but positively with the inflammatory factors *TNFA* and *IL6* in visceral fat (Figure 7, D and E). Pearson correlation analysis showed that the homeostasis model assessment of insulin resistance (HOMA-IR) was positively associated with miR-34a abundance in visceral fat (Figure 7F; $r = 0.3403$, $P < 0.05$), but negatively correlated with *KLF4* mRNA levels in the adipose tissue (Figure 7G; $r = -0.3565$, $P < 0.05$). Furthermore, when the overweight/obese subjects were classified into insulin-sensitive (HOMA-IR < 1, $n = 8$) and insulin-resistant groups (HOMA-IR > 1, $n = 16$) according to the optimal cut-off value determined in our 15-year prospective study (37), the insulin-sensitive subjects exhibited a lower level of miR-34a than those with a higher HOMA-IR value (0.89 ± 0.24 vs. 1.87 ± 0.22, $P < 0.05$).

Discussion

In the present study, we uncovered adipocyte-secreted exosomes as a potentially novel mediator of obesity-induced adipose inflammation, acting by transporting miR-34a into the adjacent macrophages, where it drives the polarization program toward proinflammatory M1 phenotype by targeting the transcription factor KLF4 (Figure 8). The miR-34a expression in visceral fat is progressively increased with the development of dietary obesity, whereas adipose-selective ablation of miR-34a protects mice from exacerbation of metainflammation and insulin resistance caused by dietary stress. The high level of miR-34a expression in visceral fat may explain in part why this adipose depot is more prone to inflammation and is closely related to insulin resistance and type 2 diabetes.

In both rodents and humans, we found that increased miR-34a expression in obese adipose tissues is closely associated with the degree of insulin resistance and metabolic inflammation. A positive correlation between adipose miR-34a expression and BMI has also been reported in several previous clinical studies (38, 39). Although the precise mechanism whereby obesity induces adipose miR-34a expression remains unknown, both our results and previous studies showed that TNF-α, a proinflammatory cytokine that is elevated at the very early stage of obesity, increases miR-34a expression (40, 41). Furthermore, in line with our results, palmitate, a toxic lipid that is increased in obesity, has been reported to induce miR-34a expression through the activation of the transcription factor Foxo3 (42). Therefore, the increased miR-34a expression in obese adipose tissue might be attributed to the synergistic effects of various metabolic stress–induced signaling cascades.

Apart from macrophages, adipose tissues contain a multitude of other immune cells, and their crosstalk plays a crucial role in maintaining the local immunometabolic homeostasis. Previous studies have identified several types of immune cells and a number of immunological factors involved in infiltration and polarization of macrophages in adipose tissues (43). In obesity, infiltration of $CD8^+$ cytotoxic T cells precedes the accumulation of macrophages in adipose tissues, and immunological and genetic depletion of $CD8^+$ T cells lowers macrophage infiltration and ameliorates adipose tissue inflammation and systemic insulin resistance (44). On the other hand, eosinophils, which account for 4%–5% of the stromal vascular fraction in healthy lean adipose tissue, promote M2 polarization of ATMs through production of IL-4 and IL-13 (12). Likewise, group 2 innate lymphoid cells (ILC2s) promote the recruitment of eosinophils and subsequent polarization of M2 ATMs by providing a major source of IL-5 and IL-13 to the adipose tissues (45). Activation of type 1 NKT cells by the lipid agonist α-galactosylceramide enhances M2 polarization of ATMs and improves glucose homeostasis in obese mice (14). However, the pathophysiological roles of these immune cells in driving M2-to-M1 transition of ATMs in obesity remain to be established. Our present study shows that the miRNA signals released from hypertrophic adipocytes can directly suppress M2 polarization of ATMs in obese mice, without the involvement of eosinophils, ILC2s, or Th2 cytokines. Indeed, a growing body of evidence suggests that adipocytes control both recruitment and polarization of ATMs through direct crosstalk between these 2 major types of cells in adipose tissues (8, 28). Ablation of SIRT1 in adipocytes, but not in macrophages per se, leads to exacerbated infiltration and activation of proinflammatory M1 ATMs, without any alteration of T cells, eosinophils, and neutrophils (46). Adipocytes, on the one hand, produce the chemokine MCP-1 to promote the recruitment of ATMs and, on the other hand, secrete adiponectin, which suppresses the infiltration but promotes alternative polarization of ATMs. In this connection, our present findings suggest adipocyte-secreted exosomal miRNAs as another important mediator whereby adipocytes control the polarization of ATMs in obesity.

The exosomes are extracellular nano-sized particles (30–100 nm in diameter) that originate from endocytosis-mediated invagination of the plasma membrane. A growing body of evidence suggests that the exosomes are an important signaling mediator for intercellular communication and interorgan crosstalk, through delivery of the exosomal cargoes to the target cells, or interaction of the exosomal signaling molecules with the cell surface receptors (47, 48). The exosomal signaling is largely determined by their composition of miRNAs, which control the gene expression in target cells by promoting mRNA degradation and blocking mRNA degradation. In both humans and mice, adipose tissue–derived exosomes are the primary source of miRNAs in the circulation (20). The miRNA content of the exosomes derived from adipocytes of human obese visceral adipose tissue differs significantly from that of lean subjects, whereas alterations in adipocyte-derived exosomal miRNAs are closely associated with decreased insulin resistance after bariatric surgery (49). The adipose-secreted exosomes play a crucial role in coordinating the communications between adipocytes and other types of cells within adipose tissues, as well as between adipose tissues and other key metabolic organs such as liver and skeletal muscle (20). Deng et al. demonstrated that injection of the exosomes purified from visceral adipose tissues of obese mice into lean mice results in glucose intolerance and insulin resistance by inducing

activation of proinflammatory macrophages (50). Furthermore, intravenous injection of the exosomes purified from visceral adipose tissues leads to a marked exacerbation of atherosclerosis in hyperlipidemic apolipoprotein E–deficient mice, due to increased foam cell formation from macrophages (51). Notably, both studies found that adipocyte-derived exosomes can directly induce the M1 polarization and production of proinflammatory cytokines from macrophages, although the specific exosomal components driving these changes remain unclear. In this connection, our present study shows that the stimulatory effect of the exosomes derived from miR-34a–deficient adipocytes on M1 macrophage polarization and production of inflammatory cytokines is largely compromised compared with that of the exosomes derived from adipocytes of WT mice, suggesting miR-34a as a crucial cargo of adipocyte-derived exosomes conferring the inflammatory responses in macrophages. In line with our findings, the secreted form of miR-34a from renal fibroblasts induces tubular cell apoptosis (52). Likewise, miR-34a is secreted via shedding vehicles of astrocytes, which in turn enhances vulnerability of dopaminergic neurons to neurotoxins by targeting the antiapoptotic protein Bcl-2 (53).

While adipocyte-secreted exosomes exert profound effects on polarization and function of ATMs, ATMs themselves also produce exosomes to regulate the metabolism and insulin actions in both local adipocytes and distal metabolic organs (35). Interestingly, the exosome-like vehicles from M1 macrophages impair insulin signaling in human adipocytes, but those from M2 macrophages exert opposite effects (54). Likewise, exosomes obtained from ATMs of lean mice improve glucose tolerance and insulin sensitivity when administered to obese mice, whereas injection of exosomes isolated from ATMs of obese mice induce glucose intolerance and insulin resistance in lean mice (35). MiR-155, a repressor of the transcription factor peroxisome proliferator–activated receptor-γ (PPARγ), has been identified as a key culprit for the effects of ATM exosomes on insulin resistance. Taken together, these findings support the notion that the exosomal miRNAs are the key players in mediating the adipocyte-macrophage crosstalk within adipose tissues in both physiological and pathophysiological conditions.

The M1/M2 polarization of macrophages is controlled by a network of transcription factors, including IFN regulatory factor (IRF), signal transducers and activators of transcription (STATs), suppressor of cytokine signaling (SOCS), and KLFs (55). KLFs are a subfamily of the zinc finger class of the transcriptional regulators. KLF4, which is one of the 4 well-defined transcription factors for generating pluripotent stem cells, promotes M2 macrophage polarization as well as monocyte differentiation (56, 57). KLF4-deficient macrophages exhibit impaired IL-4–induced M2 polarization, whereas overexpression of KLF4 in RAW264.7 macrophages induces IL-4–mediated M2 gene expression (58). Mechanistically, IL-4 increases KLF4 expression by phosphorylation of STAT6, and these 2 transcription factors in turn cooperate to induce the expression of a set of genes functionally related to the M2 macrophage phenotype (56). Furthermore, KLF4 induces the macrophagic expression of MCP-1–induced protein (MCPIP), which in turn promotes M2 polarization through its deubiquitinase and RNase activities (59). In the present study, we provide a series of evidence demonstrating that miR-34a–mediated downregulation of KLF4 is an important driver for reduced M2 polarization of ATMs in obesity, which in turn triggers metabolic inflammation and insulin resistance. In visceral adipose tissues of both rodents and humans with overweight/obesity, increased miR-34a expression is closely associated with reduced KLF4 expression. Furthermore, overexpression of KLF4 is sufficient to counteract obesity-induced reduction of M2 polarization of ATMs in obese mice as well as miR-34a–mediated suppression of IL-4–induced M2 polarization of bone marrow–derived macrophages. Consistently, myeloid-specific deletion of KLF4 exacerbates dietary obesity–induced glucose intolerance and insulin resistance, and causes delayed wound healing due to defective M2 macrophage polarization (56).

Adipose-resident M1 macrophages contribute to obesity-related insulin resistance and glucose intolerance by releasing proinflammatory cytokines, which in turn act either in an autocrine/paracrine manner to modulate the functions of adipose tissues, or in an endocrine manner to impair insulin actions in distal organs such as liver and skeletal muscle (60). Furthermore, M1 macrophages are also important players in obesity-induced remodeling of extracellular matrix in adipose tissues, by augmenting collagen formation and fibrosis (61). Adipose fibrosis is causally associated with obesity-related systemic insulin resistance and metabolic disturbance by compromising the flexibility of the tissues for healthy expansion, thereby leading to ectopic lipid accumulation, as well as by exacerbating adipocyte dysfunction, aberrant adipokine production, and metabolic inflammation. Mice lacking collagen VI, a major component of extracellular matrix proteins in adipose tissues, exhibit increased adipose expansion due to attenuated fibrosis, accompanied by reduced adipose inflammation and improved insulin sensitivity compared with WT littermates (62). Consistently, our present study observed a marked attenuation in HFD-induced collagen formation and expression of fibrotic genes in epiWAT of the miR-34a–KO mice despite increased fat mass, suggesting that miR-34a is also an important contributor to obesity-induced adipose fibrosis by regulating macrophage properties. Furthermore, we found that circulating adiponectin, a major adipocyte-derived adipokine with insulin-sensitizing activity, is much higher in miR-34a–KO mice than in WT littermates on HFD, whereas such a difference in adiponectin between the 2 groups is abrogated by macrophage ablation, indicating that miR-34a suppresses adiponectin production indirectly through modulation of macrophages. Taken together, the obvious amelioration of obesity-associated insulin resistance and glucose dysregulation in the adipose-specific miR-34a–KO mice may be attributed to increased adiponectin, decreased adipose fibrosis, and reduced local and systemic inflammation, resulting from enhanced macrophage polarization from proinflammatory M1 into antiinflammatory M2 phenotype (Figure 8).

Like most other miRNAs, miR-34a regulates the expression of multiple genes in different tissues. In the heart tissue, miR-34a is induced by aging and contributes to aging-related decline in cardiac function and cardiac cell death by downregulation of PNUTS, which reduces telomere shortening (63). In endothelial cells, miR-34a induces apoptosis by downregulation of Bcl2, thereby resulting in endothelial dysfunction and accelerated atherosclerosis in apolipoprotein E-deficient (apoE$^{-/-}$) mice (64). Notably, several

recent studies by Kemper and colleagues demonstrated that miR-34a impairs the metabolic actions of FGF19/FGF21 by inhibiting the expression of β-klotho, an obligate coreceptor for both hormones. Treatment of dietary-obese mice with antisense RNA for miR-34a (anti–miR-34a) restores hepatic β-klotho expression and FGF19 signaling, leading to attenuation of fatty liver disease (23, 65). Furthermore, miR-34a reduces NAD^+ levels and impairs the activity of the anti-aging molecule SirT1 by downregulation of nicotinamide phosphoribosyltransferase (NAMPT), the rate-limiting enzyme for NAD^+ biosynthesis (66). Taken together, these findings suggest that elevated miR-34a is a culprit for a cluster of obesity-related cardiometabolic diseases through its actions in multiple targets in different organs. Pharmacological or genetic inhibition of miR-34a may represent a promising therapeutic strategy for these chronic disorders.

There are several limitations to this study. First, in light of the fact that recruitment and polarization of adipose-resident macrophages are a complex process regulated by a plethora of metabolic and immunological factors, it remains to be determined whether and how miR-34a communicates and coordinates with other regulators to control the number and properties of adipose-resident macrophages during the development of obesity. Second, although we found much higher expression of miR-34a in visceral WAT than subcutaneous WAT in both rodents and humans, our current study cannot address the adipose depot–specific regulation and functions of miR-34a because of the lack of genetically modified rodent models with adipose depot–specific gene ablation. Further studies on these issues will help us to understand the molecular basis of the heterogeneity of subcutaneous and visceral WAT.

Methods

For a detailed description of all methods, see Supplemental Methods online.

Mice. MiR-34a$^{fl/fl}$ mice, in which LoxP sites flank the entire miR-34a sequence, were purchased from The Jackson Laboratory and backcrossed with C57BL/6J background for at least 10 generations. Adipose- or adipocyte-specific miR-34a–KO mice were generated by crossing of *aP2*-Cre or *adiponectin*-Cre transgenic mice with miR-34a$^{fl/fl}$ mice on C57BL/6J background. MiR-34a–KO mice and their WT littermates (miR-34a$^{fl/fl}$ mice) were maintained on 12-hour light/12-hour dark cycles under controlled environmental settings (23°C ± 1°C), with free access to water. Four-week-old male mice were fed with STC (13% of calories from fat, D5053; LabDiet) or HFD (60% of calories from fat, D12492; Research Diet) for various time periods.

Glucose tolerance and insulin tolerance tests. For glucose tolerance test, mice fasted for 15 hours were challenged with D-glucose (1 g/kg body weight) by oral gavage. Blood glucose levels in tail vein were monitored at various time points (0, 15, 30, 60, 90, and 120 minutes) after glucose infusion with a OneTouch Glucose Meter (LifeScan). For insulin tolerance test, mice fasted for 5 hours were intraperitoneally injected with insulin (0.5 or 0.75 IU/kg body weight for STC- or HFD-fed mice, respectively), followed by measurement of blood glucose as above.

Biochemical and immunological measurement of circulating parameters. Serum levels of insulin (no. 32100), adiponectin (no. 32010), and FGF21 (no. 32180) were determined by mouse high-sensitive ELISA kits (Immunodiagnostics, Hong Kong). Circulating levels of soluble TNF-α (MTA00B), IL-6 (M6000B), IL-1β (MLB00C), and MCP-1 (DY479) were quantified by ELISA kits (R&D Systems). Serum triglyceride level was analyzed with a biochemical assay kit (Stanbio Laboratory).

Human subjects. Fifty-three premenopausal adult Chinese women, including 29 lean individuals with BMI less than 23 kg/m^2 and 24 overweight/obese subjects with BMI of at least 23 kg/m^2, undergoing elective abdominal surgery for benign, noninfective gynecological conditions were recruited at Queen Mary Hospital, University of Hong Kong (67). The clinical characteristics of these study participants were described in our previous report (67). Homeostasis model assessment (HOMA) index was calculated as fasting glucose (mM) × fasting insulin (mIU/liter)/22.5. During the operation, visceral adipose tissues (~8 cm^3 each) were collected aseptically and immediately subjected to total RNA extraction.

Statistics. Data are expressed as means ± SEM. All analyses were performed with Prism 5 (GraphPad Software Inc.). Comparison between groups was performed using ANOVA or the 2-tailed Student's *t* test as appropriate. Correlations between different gene expressions and insulin resistance index were examined by Pearson correlation analysis. In all statistical comparisons, a *P* value less than 0.05 was considered significant.

Study approval. All animal experimental procedures were approved by the Committee on the Use of Live Animals in Teaching and Research at the University of Hong Kong. The human studies were approved by the human ethics committees of the University of Hong Kong. Written informed consent was received from participants prior to their inclusion in the study.

Author contributions

YP designed and performed the experiments, analyzed the results, and wrote the manuscript. XH and RLCH discussed the results. DY performed the experiments. CYCC performed the experiments and analyzed the data. TF generated recombinant viruses for this study. YW edited the manuscript. KSLL provided clinical samples and reviewed the manuscript. AX designed the study and wrote and edited the manuscript.

Acknowledgments

This work was supported by the Hong Kong Research Grants Council Collaborative Research Fund (C7055-14G, C7037-17W), the Health and Medical Research Fund (02132836), and the HKU matching fund for the State Key Laboratory of Pharmaceutical Biotechnology.

Address correspondence to: Aimin Xu, the University of Hong Kong, L8-40, 21 Sassoon Road, New Laboratory Block, Pokfulam, Hong Kong. Phone: 852.39179754; Email: amxu@hku.hk.

1. Scherer PE. Adipose tissue: from lipid storage compartment to endocrine organ. *Diabetes*. 2006;55(6):1537–1545.
2. Rosen ED, Spiegelman BM. What we talk about when we talk about fat. *Cell*. 2014;156(1–2):20–44.
3. Zhang X, et al. Selective inactivation of c-Jun NH2-terminal kinase in adipose tissue protects against diet-induced obesity and improves insulin sensitivity in both liver and skeletal muscle in mice. *Diabetes*. 2011;60(2):486–495.
4. Murray PJ. The primary mechanism of the IL-10-regulated antiinflammatory response is to selectively inhibit transcription. *Proc Natl Acad Sci U S A*. 2005;102(24):8686–8691.
5. Weisberg SP, McCann D, Desai M, Rosenbaum M,

Leibel RL, Ferrante AW. Obesity is associated with macrophage accumulation in adipose tissue. *J Clin Invest*. 2003;112(12):1796–1808.
6. Cinti S, et al. Adipocyte death defines macrophage localization and function in adipose tissue of obese mice and humans. *J Lipid Res*. 2005;46(11):2347–2355.
7. Shi H, Kokoeva MV, Inouye K, Tzameli I, Yin H, Flier JS. TLR4 links innate immunity and fatty acid-induced insulin resistance. *J Clin Invest*. 2006;116(11):3015–3025.
8. Lumeng CN, Bodzin JL, Saltiel AR. Obesity induces a phenotypic switch in adipose tissue macrophage polarization. *J Clin Invest*. 2007;117(1):175–184.
9. Sica A, Mantovani A. Macrophage plasticity and polarization: in vivo veritas. *J Clin Invest*. 2012;122(3):787–795.
10. Odegaard JI, et al. Macrophage-specific PPARgamma controls alternative activation and improves insulin resistance. *Nature*. 2007;447(7148):1116–1120.
11. Kang K, et al. Adipocyte-derived Th2 cytokines and myeloid PPARdelta regulate macrophage polarization and insulin sensitivity. *Cell Metab*. 2008;7(6):485–495.
12. Wu D, et al. Eosinophils sustain adipose alternatively activated macrophages associated with glucose homeostasis. *Science*. 2011;332(6026):243–247.
13. Tiemessen MM, Jagger AL, Evans HG, van Herwijnen MJ, John S, Taams LS. $CD4^+CD25^+Foxp3^+$ regulatory T cells induce alternative activation of human monocytes/macrophages. *Proc Natl Acad Sci U S A*. 2007;104(49):19446–19451.
14. Ji Y, et al. Activation of natural killer T cells promotes M2 Macrophage polarization in adipose tissue and improves systemic glucose tolerance via interleukin-4 (IL-4)/STAT6 protein signaling axis in obesity. *J Biol Chem*. 2012;287(17):13561–13571.
15. Bartel DP. MicroRNAs: genomics, biogenesis, mechanism, and function. *Cell*. 2004;116(2):281–297.
16. Bartel DP. MicroRNAs: target recognition and regulatory functions. *Cell*. 2009;136(2):215–233.
17. Kasinski AL, Slack FJ. Epigenetics and genetics. MicroRNAs en route to the clinic: progress in validating and targeting microRNAs for cancer therapy. *Nat Rev Cancer*. 2011;11(12):849–864.
18. Rottiers V, Näär AM. MicroRNAs in metabolism and metabolic disorders. *Nat Rev Mol Cell Biol*. 2012;13(4):239–250.
19. Arner P, Kulyté A. MicroRNA regulatory networks in human adipose tissue and obesity. *Nat Rev Endocrinol*. 2015;11(5):276–288.
20. Thomou T, et al. Adipose-derived circulating miRNAs regulate gene expression in other tissues. *Nature*. 2017;542(7642):450–455.
21. Klöting N, et al. MicroRNA expression in human omental and subcutaneous adipose tissue. *PLoS One*. 2009;4(3):e4699.
22. Ortega FJ, et al. MiRNA expression profile of human subcutaneous adipose and during adipocyte differentiation. *PLoS One*. 2010;5(2):e9022.
23. Fu T, et al. MicroRNA 34a inhibits beige and brown fat formation in obesity in part by suppressing adipocyte fibroblast growth factor 21 signaling and SIRT1 function. *Mol Cell Biol*. 2014;34(22):4130–4142.
24. Sun K, et al. Endotrophin triggers adipose tissue fibrosis and metabolic dysfunction. *Nat Commun*. 2014;5:3485.
25. Brestoff JR, et al. Group 2 innate lymphoid cells promote beiging of white adipose tissue and limit obesity. *Nature*. 2015;519(7542):242–246.
26. Takeda K, Kamanaka M, Tanaka T, Kishimoto T, Akira S. Impaired IL-13-mediated functions of macrophages in STAT6-deficient mice. *J Immunol*. 1996;157(8):3220–3222.
27. Shimoda K, et al. Lack of IL-4-induced Th2 response and IgE class switching in mice with disrupted Stat6 gene. *Nature*. 1996;380(6575):630–633.
28. Lumeng CN, Deyoung SM, Bodzin JL, Saltiel AR. Increased inflammatory properties of adipose tissue macrophages recruited during diet-induced obesity. *Diabetes*. 2007;56(1):16–23.
29. Oh DY, Morinaga H, Talukdar S, Bae EJ, Olefsky JM. Increased macrophage migration into adipose tissue in obese mice. *Diabetes*. 2012;61(2):346–354.
30. Hui X, et al. Adiponectin enhances cold-induced browning of subcutaneous adipose tissue via promoting M2 macrophage proliferation. *Cell Metab*. 2015;22(2):279–290.
31. Patsouris D, Li PP, Thapar D, Chapman J, Olefsky JM, Neels JG. Ablation of CD11c-positive cells normalizes insulin sensitivity in obese insulin resistant animals. *Cell Metab*. 2008;8(4):301–309.
32. Lee YS, et al. Inflammation is necessary for long-term but not short-term high-fat diet-induced insulin resistance. *Diabetes*. 2011;60(10):2474–2483.
33. Betel D, Koppal A, Agius P, Sander C, Leslie C. Comprehensive modeling of microRNA targets predicts functional non-conserved and non-canonical sites. *Genome Biol*. 2010;11(8):R90.
34. Yuan A, et al. Transfer of microRNAs by embryonic stem cell microvesicles. *PLoS One*. 2009;4(3):e4722.
35. Ying W, et al. Adipose tissue macrophage-derived exosomal miRNAs can modulate in vivo and in vitro insulin sensitivity. *Cell*. 2017;171(2):372–384.e12.
36. Kowal J, et al. Proteomic comparison defines novel markers to characterize heterogeneous populations of extracellular vesicle subtypes. *Proc Natl Acad Sci U S A*. 2016;113(8):E968–E977.
37. Lee CH, et al. Optimal cut-offs of homeostasis model assessment of insulin resistance (HOMA-IR) to identify dysglycemia and type 2 diabetes mellitus: a 15-year prospective study in Chinese. *PLoS One*. 2016;11(9):e0163424.
38. Lavery CA, et al. miR-34a(–/–) mice are susceptible to diet-induced obesity. *Obesity (Silver Spring)*. 2016;24(8):1741–1751.
39. Lu H, et al. Elevated circulating stearic acid leads to a major lipotoxic effect on mouse pancreatic β cells in hyperlipidaemia via a miR-34a-5p-mediated PERK/p53-dependent pathway. *Diabetologia*. 2016;59(6):1247–1257.
40. Akca H, Yenisoy S, Yanikoglu A, Ozes ON. Tumor necrosis factor-alpha-induced accumulation of tumor suppressor protein p53 and cyclin-dependent protein kinase inhibitory protein p21 is inhibited by insulin in ME-180S cells. *Clin Chem Lab Med*. 2002;40(8):764–768.
41. Wu H, Lozano G. NF-κB activation of p53. A potential mechanism for suppressing cell growth in response to stress. *J Biol Chem*. 1994;269(31):20067–20074.
42. Natarajan SK, et al. FoxO3 increases miR-34a to cause palmitate-induced cholangiocyte lipoapoptosis. *J Lipid Res*. 2017;58(5):866–875.
43. Schipper HS, Prakken B, Kalkhoven E, Boes M. Adipose tissue-resident immune cells: key players in immunometabolism. *Trends Endocrinol Metab*. 2012;23(8):407–415.
44. Nishimura S, et al. $CD8^+$ effector T cells contribute to macrophage recruitment and adipose tissue inflammation in obesity. *Nat Med*. 2009;15(8):914–920.
45. Molofsky AB, et al. Innate lymphoid type 2 cells sustain visceral adipose tissue eosinophils and alternatively activated macrophages. *J Exp Med*. 2013;210(3):535–549.
46. Hui X, et al. Adipocyte SIRT1 controls systemic insulin sensitivity by modulating macrophages in adipose tissue. *EMBO Rep*. 2017;18(4):645–657.
47. Denzer K, Kleijmeer MJ, Heijnen HF, Stoorvogel W, Geuze HJ. Exosome: from internal vesicle of the multivesicular body to intercellular signaling device. *J Cell Sci*. 2000;113(pt 19):3365–3374.
48. Valadi H, Ekström K, Bossios A, Sjöstrand M, Lee JJ, Lötvall JO. Exosome-mediated transfer of mRNAs and microRNAs is a novel mechanism of genetic exchange between cells. *Nat Cell Biol*. 2007;9(6):654–659.
49. Hubal MJ, et al. Circulating adipocyte-derived exosomal microRNAs associated with decreased insulin resistance after gastric bypass. *Obesity (Silver Spring)*. 2017;25(1):102–110.
50. Deng ZB, et al. Adipose tissue exosome-like vesicles mediate activation of macrophage-induced insulin resistance. *Diabetes*. 2009;58(11):2498–2505.
51. Xie Z, et al. Adipose-derived exosomes exert proatherogenic effects by regulating macrophage foam cell formation and polarization. *J Am Heart Assoc*. 2018;7(5):e007442.
52. Zhou Y, et al. Secreted fibroblast-derived miR-34a induces tubular cell apoptosis in fibrotic kidney. *J Cell Sci*. 2014;127(pt 20):4494–4506.
53. Mao S, Sun Q, Xiao H, Zhang C, Li L. Secreted miR-34a in astrocytic shedding vesicles enhanced the vulnerability of dopaminergic neurons to neurotoxins by targeting Bcl-2. *Protein Cell*. 2015;6(7):529–540.
54. Zhang Y, et al. Inflamed macrophage microvesicles induce insulin resistance in human adipocytes. *Nutr Metab (Lond)*. 2015;12:21.
55. Lawrence T, Natoli G. Transcriptional regulation of macrophage polarization: enabling diversity with identity. *Nat Rev Immunol*. 2011;11(11):750–761.
56. Liao X, et al. Krüppel-like factor 4 regulates macrophage polarization. *J Clin Invest*. 2011;121(7):2736–2749.
57. Feinberg MW, et al. The Kruppel-like factor KLF4 is a critical regulator of monocyte differentiation. *EMBO J*. 2007;26(18):4138–4148.
58. Liu J, Liu Y, Zhang H, Chen G, Wang K, Xiao X. KLF4 promotes the expression, translocation, and releas eof HMGB1 in RAW264.7 macrophages in response to LPS. *Shock*. 2008;30(3):260–266.
59. Kapoor N, et al. Transcription factors STAT6 and KLF4 implement macrophage polarization via the dual catalytic powers of MCPIP. *J Immunol*. 2015;194(12):6011–6023.

60. Osborn O, Olefsky JM. The cellular and signaling networks linking the immune system and metabolism in disease. *Nat Med*. 2012;18(3):363–374.
61. Spencer M, et al. Adipose tissue macrophages in insulin-resistant subjects are associated with collagen VI and fibrosis and demonstrate alternative activation. *Am J Physiol Endocrinol Metab*. 2010;299(6):E1016–E1027.
62. Khan T, et al. Metabolic dysregulation and adipose tissue fibrosis: role of collagen VI. *Mol Cell Biol*. 2009;29(6):1575–1591.
63. Boon RA, et al. MicroRNA-34a regulates cardiac ageing and function. *Nature*. 2013;495(7439):107–110.
64. Su G, Sun G, Liu H, Shu L, Liang Z. Downregulation of miR-34a promotes endothelial cell growth and suppresses apoptosis in atherosclerosis by regulating Bcl-2. *Heart Vessels*. 2018;33(10):1185–1194.
65. Fu T, et al. Aberrantly elevated microRNA-34a in obesity attenuates hepatic responses to FGF19 by targeting a membrane coreceptor β-Klotho. *Proc Natl Acad Sci U S A*. 2012;109(40):16137–16142.
66. Choi SE, et al. Elevated microRNA-34a in obesity reduces NAD+ levels and SIRT1 activity by directly targeting NAMPT. *Aging Cell*. 2013;12(6):1062–1072.
67. Zhang X, et al. Serum FGF21 levels are increased in obesity and are independently associated with the metabolic syndrome in humans. *Diabetes*. 2008;57(5):1246–1253.